Article:

Dell, A., Krynkin, A. and Horoshenkov, K.V. orcid.org/0000-0002-6188-0369 (2021) The use of the transfer matrix method to predict the effective fluid properties of acoustical systems. Applied Acoustics, 182. 108259. ISSN 0003-682X

https://doi.org/10.1016/j.apacoust.2021.108259

Applied Acoustics 182 (2021) 108259

Contents lists available at ScienceDirect

Applied Acoustics

journal homepage: www.elsevier.com/locate/apacoust

The use of the transfer matrix method to predict the effective fluid properties of acoustical systems

A. Dell *, A. Krynkin, K.V. Horoshenkov

The University of Sheffield, Department of Mechanical Engineering, Sheffield S1 3JD, United Kingdom

ARTICLE INFO

Article history:
Received 21 December 2020
Received in revised form 21 May 2021
Accepted 18 June 2021

Keywords:
Transfer matrix method
Effective properties
Waveguide
Tortuous pore
Helmholtz resonator
Sound absorption

ABSTRACT

The transfer matrix method (TMM) is a common method for the modelling of acoustical systems. Traditionally, this method requires each unique layer within a system to be defined by a transfer matrix and then for each matrix to be multiplied together in the sequential order of the system. Whilst the resulting matrix can be used to find the effective material properties of the modelled system, the resulting analytical expressions of these properties are often unwieldy for use. Here, a simplified approach is proposed to obtain simple analytical expressions in the low frequency regime for the effective properties of acoustical systems based on the components of the TMM and inspired by the Champoux and Stinson model. It was shown that the proposed approximation of TMM matches the effective fluid properties of a cylindrical rigid tortuous pore derived with the Champoux and Stinson model. Using this approach, analytical expressions for the effective fluid properties of a waveguide of constant cross section, side-loaded by an arbitrary number of Helmholtz resonators, were derived. These expressions were validated against the traditional transfer matrix method and with numerical computation. The result of this work offers a validated general approach that provides simple analytical low frequency approximations of the acoustical properties of media which consist of complicated networks of pores or side-branches.

1. Introduction

The transfer matrix method (TMM) is a simple and powerful method to model acoustical systems. Using this method it is possible to analyse the sound absorption/transmission properties of one and two port systems [1], assess effects due to periodicity [2,3] and derive effective property expressions for porous layers [4]. Additionally, it has proven to be a popular technique in order to model multilayered porous materials [5], parallel assemblies of porous materials [6] and sound absorbing acoustic metamaterials consisting of waveguide structures side-loaded by Helmholtz resonators [7,8].

In the acoustics of porous materials, sound propagation in rigid tortuous pores is modelled with the linear superposition of the macroscopic pressure gradient and the averaged velocity within pore segments of constant cross-section. This approach of discretising pores into segments was used in the Champoux and Stinson model [9] to determine the effective density and compressibility and thus enables the building of simple acoustical models.

In this paper, a general methodology is proposed to obtain simple analytical expressions for the effective material properties for systems that can be modelled with the TMM. The proposed method utilises the linear superposition of terms derived from the transfer matrix components of a system to obtain the total effective properties of the system. This method differs from the traditional transfer matrix method as it is not reliant upon the matrix multiplication of each segment's transfer matrices. As such, simple analytical expressions for complex systems can be derived using this method, allowing for an insight into the underlying physics of these systems.

The proposed methodology is validated for two scenarios. Firstly, the effective properties are obtained for a single rigid tortuous pore consisting of cylindrical sections of varying cross sectional area. The obtained effective properties are simplified to succinct analytical expressions which match the well established Champoux and Stinson model [9]. These expressions are validated against the traditional TMM. Secondly, simple general expressions for the effective dynamic density and complex compressibility are obtained for a waveguide side-loaded by an arbitrary number of Helmholtz resonators. These expressions are validated against results obtained using the traditional TMM and numerically.

* Corresponding author.
E-mail address: ajdell1@sheffield.ac.uk (A. Dell).

https://doi.org/10.1016/j.apacoust.2021.108259
0003-682X/

The paper is organised as follows. All the required supplementary theory is presented in Section 2. The TMM and linear superposition approach are bridged together to express the effective properties of an acoustical system in Section 3. The proposed model is compared with the traditional TMM for a rigid tortuous pore in Section 4 and with a waveguide sideloaded with Helmholtz resonators in Section 5.

2. Background theory

2.1. Basic equations

Consider a one-dimensional harmonic plane wave with $e^{i\omega t}$ time dependence, where $i = \sqrt{-1}$, which propagates in a duct of stationary ideal gas with a cross sectional area S_a. The macroscopic pressure gradient $-\partial p/\partial x$ is applied to a medium in the x direction, where p is the complex acoustic pressure amplitude at any point. The equation of motion is written as follows [9]:

$$-\frac{\partial p}{\partial x} = i\omega\rho(\omega)v, \tag{1}$$

where $\rho(\omega)$ is the effective frequency dependent dynamic fluid density, ω is the angular frequency and v is the complex average macroscopic fluid velocity in the x direction. For a small perturbation in the medium, the following expressions can be written based on the continuity and thermodynamic state equations [9], respectively:

$$\rho_0\frac{\partial v}{\partial x} + i\omega\delta\rho = 0, \tag{2}$$

$$\frac{\delta\rho}{\rho_0} = C(\omega)p. \tag{3}$$

Here we adopt notations similar to those used in Ref. [9] so that ρ_0 is the equilibrium density, $\delta\rho$ is the perturbation density and $C(\omega)$ is the effective complex compressibility of the fluid. Note that the effective bulk modulus $K(\omega)$ is simply the inverse of the complex compressibility, i.e. $1/C(\omega)$. The combination of Eqs. (2) and (3) leads to:

$$-\frac{\partial v}{\partial x} = i\omega C(\omega)p. \tag{4}$$

Subsequently, the effective dynamic fluid density and complex compressibility can be used to obtain the characteristic impedance, $Z(\omega)$, and acoustic wavenumber, $k(\omega)$, respectively:

$$Z(\omega) = \frac{1}{S_a}\sqrt{\frac{\rho(\omega)}{C(\omega)}}, \tag{5}$$

$$k(\omega) = \omega\sqrt{\rho(\omega)C(\omega)}. \tag{6}$$

The speed of sound, $c(\omega)$, can then be found simply as:

$$c(\omega) = [\rho(\omega)C(\omega)]^{-1/2}. \tag{7}$$

2.2. Viscothermal losses

Viscothermal losses within a duct are accounted for by evaluating the complex frequency dependent density and bulk modulus for a plane wave propagating through a section of constant cross section [10]. For a circular duct of radius r:

$$\rho(\omega) = \rho_0\left[1 - \frac{2J_1(rG_r)}{rG_rJ_0(rG_r)}\right], \tag{8}$$

$$K(\omega) = K_0\left[1 + (\gamma - 1)\frac{2J_1(rG_k)}{rG_kJ_0(rG_k)}\right]. \tag{9}$$

Here $G_r = \sqrt{-i\omega\rho_0/\eta}$ and $G_k = \sqrt{-i\omega\rho_0 Pr/\eta}$, in which ρ_0 is the equilibrium density, $K_0 = \gamma P_0$ is the adiabatic bulk modulus, γ is the ratio of specific heats, P_0 is the equilibrium pressure, Pr is the Prandtl number and η is the dynamic viscosity.

For a rectangular duct of width, a, and height, b:

$$\rho(\omega) = -\frac{\rho_0 a^2 b^2}{4G_\rho^2\sum_{k=0}^{\infty}\sum_{m=0}^{\infty}\left[\alpha_k^2\beta_m^2\left(\alpha_k^2 + \beta_m^2 - G_\rho^2\right)\right]^{-1}}, \tag{10}$$

$$K(\omega) = \frac{K_0}{\gamma + 4(\gamma-1)G_K^2/a^2b^2\sum_{k=0}^{\infty}\sum_{m=0}^{\infty}\left[\alpha_k^2\beta_m^2\left(\alpha_k^2 + \beta_m^2 - G_K^2\right)\right]^{-1}}, \tag{11}$$

where $G_\rho = \sqrt{i\omega\rho_0/\eta}, G_K = \sqrt{i\omega\rho_0 Pr/\eta}, \alpha_k = 2(k+1/2)\pi/a$ and $\beta_m = 2(m+1/2)\pi/b$. The infinite sums are computed numerically with a truncation number of 100 and an accuracy of 5 significant figures for a range of duct dimensions. Using these expressions it is then possible to calculate the characteristic impedance and acoustic wavenumber for a fluid layer.

2.3. Champoux and Stinson model for rigid frame porous materials

The methodology developed in this paper is validated against the model of rigid frame porous materials by Champoux and Stinson [9] which is recalled in this section. Consider a bulk sample of identical pores with total cross section S and total length L. Here L is sufficiently large to cover all variation of pore cross section. Within a single pore, there are M segments. Each segment, m, has a length $l^{(m)}$ and an area $S_a^{(m)}$. A schematic of a single tortuous pore can be seen in Fig. 1. It has been shown from the linear superposition of terms within each segment that the effective dynamic

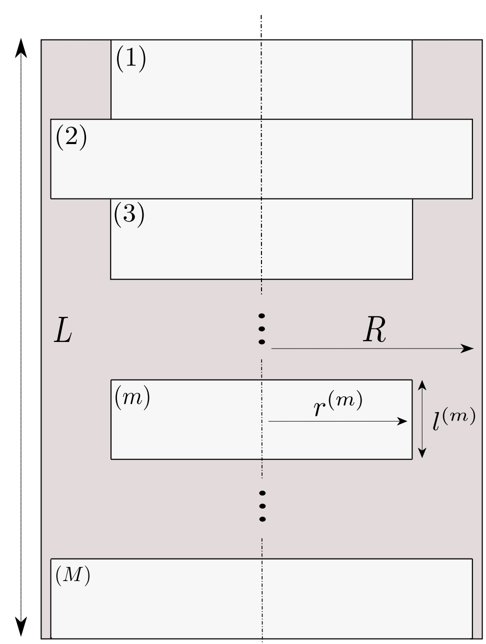

Fig. 1. Schematic of a sample containing a single tortuous pore.

density $\rho_{eff}(\omega)$ and complex compressiblity $C_{eff}(\omega)$ can be obtained as follows [9]:

$$\rho_{eff}(\omega) = \alpha_\infty \frac{\sum_{m=1}^{M} \rho(\omega)^{(m)} l^{(m)}/S_a^{(m)}}{\sum_{m=1}^{M} l^{(m)}/S_a^{(m)}}, \quad (12)$$

$$C_{eff}(\omega) = \frac{\sum_{m=1}^{M} C(\omega)^{(m)} S_a^{(m)} l^{(m)}}{\sum_{m=1}^{M} S_a^{(m)} l^{(m)}}. \quad (13)$$

Provided the geometry, dynamic density and complex compressibility are known for each pore section, it is possible to obtain the effective properties for the total system. Finally, the characteristic impedance of the bulk material is given by

$$Z_{eff}(\omega) = \frac{1}{\Omega S}\left[\frac{\rho_{eff}(\omega)}{C_{eff}(\omega)}\right]^{1/2}, \quad (14)$$

where $\Omega = \sum_{m=1}^{M} S_a^{(m)} l^{(m)}/(SL)$ is the porosity of the sample.

2.4. The transfer matrix method

2.4.1. Basic formulation

The transfer matrix method (TMM) provides the relationship between the initial sound pressure, p, and volume flux, $V = vS_a$, where S_a is the cross sectional area, at the start ($x = 0$) and at the end ($x = L$) of a medium in a duct [5]. To differentiate between the initial and end properties, the subscripts 0 and L are used, respectively. The transfer matrix, T, is derived under the assumption that only plane waves propagate through the medium in the x direction, meaning it provides the solution for a 1D wave propagation problem. The general formulation of the transfer matrix is as follows;

$$\begin{bmatrix} p \\ V \end{bmatrix}_{x=o} = T\begin{bmatrix} p \\ V \end{bmatrix}_{x=L} = \begin{bmatrix} T_{11} & T_{12} \\ T_{21} & T_{22} \end{bmatrix}\begin{bmatrix} p \\ V \end{bmatrix}_{x=L}. \quad (15)$$

This is graphically depicted for a single fluid layer within Fig. 2. The transfer matrix for a single fluid layer is constructed as

$$\begin{bmatrix} p \\ V \end{bmatrix}_{x=o} = \begin{bmatrix} \cos(kL) & iZ\sin(kL) \\ \frac{i}{Z}\sin(kL) & \cos(kL) \end{bmatrix}\begin{bmatrix} p \\ V \end{bmatrix}_{x=L} = \begin{bmatrix} T_{11} & T_{12} \\ T_{21} & T_{22} \end{bmatrix}\begin{bmatrix} p \\ V \end{bmatrix}_{x=L}. \quad (16)$$

Here, $Z = \rho c/S_a$ is the characteristic impedance, k is the acoustic wavenumber and L is the length of the fluid layer. For a multilayered structure, as shown in Fig. 3, the relationship between the input and output pressure and acoustic flux are obtained by the multiplication of the transfer matrices of each layer. This is expressed as

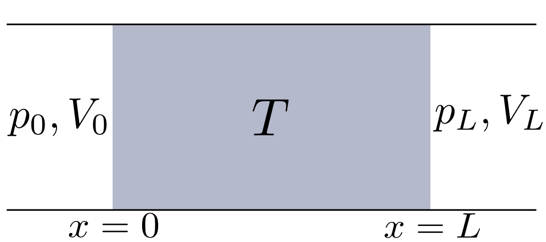

Fig. 2. Graphical depiction of the TMM applied to a single fluid layer.

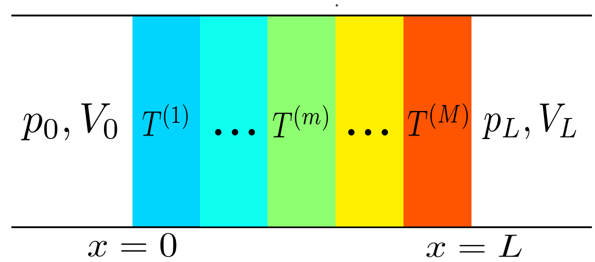

Fig. 3. Graphical depiction of the TMM approach applied to a multilayered fluid.

$$T = \prod_{m=1}^{M} T^{(m)}, \quad (17)$$

where M denotes the total amount of layers.

2.4.2. Effective material properties through TMM multiplication

Consider the transfer matrix that is the result of a series of matrix multiplications to model a system of many layers. The result is a 2x2 matrix which can be thought of as a single effective fluid layer of finite length, L. From this, the four transfer matrix elements can be directly related to the effective fluid properties [4]. Specifically, the effective wavenumber can be found as

$$k_{eff}(\omega) = \frac{1}{L}\arcsin\left(\sqrt{-T_{12}T_{21}}\right), \quad (18)$$

and the characteristic impedance as

$$Z_{eff}(\omega) = \sqrt{T_{12}/T_{21}}. \quad (19)$$

From these two equations, the effective dynamic density and complex compressibility can be obtained.

2.4.3. Transmission properties of an acoustical system using TMM

For a non-isotropic and asymmetric system, where the transmission and reflection of the incident plane wave are dependent on the direction of entry to the system, expressions can be obtained for the transmission, reflection and absorption coefficients [4]. When the incident wave propagates in the $-ikx$ direction, these are:

$$R^- = \frac{T_{11} + T_{12}/Z_0 - Z_0 T_{21} - T_{22}}{T_{11} + T_{12}/Z_0 + Z_0 T_{21} + T_{22}}. \quad (20)$$

$$T^- = \frac{2e^{ikL}}{T_{11} + T_{12}/Z_0 + Z_0 T_{21} + T_{22}}, \quad (21)$$

$$\alpha^- = 1 - |R^-|^2 - |T^-|^2. \quad (22)$$

Similarly, when the incident wave propagates in the ikx direction, these are:

$$R^+ = \frac{-T_{11} + T_{12}/Z_0 - Z_0 T_{21} + T_{22}}{T_{11} + T_{12}/Z_0 + Z_0 T_{21} + T_{22}}. \quad (23)$$

$$T^+ = \frac{2e^{ikL}(T_{11}T_{22} - T_{12}T_{21})}{T_{11} + T_{12}/Z_0 + Z_0 T_{21} + T_{22}}, \quad (24)$$

$$\alpha^+ = 1 - |R^+|^2 - |T^+|^2. \quad (25)$$

Here, Z_0 is the characteristic impedance of the surrounding medium. Furthermore, if a system is isotropic and homogeneous, then the layer is reciprocal. As such, the determinant of the transfer matrix is equal to unity. i.e.:

$$T_{11}T_{22} - T_{21}T_{12} = 1. \quad (26)$$

Additionally, if the system is symmetric, i.e. the reflection coefficient is independent of the direction of wave propagation, then the following condition holds true:

$$T_{11} = T_{22}. \tag{27}$$

From these conditions, it is evident that if the system becomes isotropic and symmetric, then Eqs. (21)–(23) reduce to $T^+ = T^-$ and $R^+ = R^-$. i.e. The acoustic transmission and reflective properties of the system are independent on the direction of incidence. This leads to the following transmission and reflection coefficients:

$$T = \frac{2e^{ikL}}{T_{11} + T_{12}/Z_0 + Z_0T_{21} + T_{22}}, \tag{28}$$

$$R = \frac{T_{11} + T_{12}/Z - Z_0T_{21} - T_{22}}{T_{11} + T_{12}/Z_0 + Z_0T_{21} + T_{22}}. \tag{29}$$

2.4.4. Obtaining the impedance of a Helmholtz resonator using the TMM

The methodology developed in this paper can be applied to derive effective properties of a waveguide side loaded with Helmholtz resonators (see Fig. 6 for clarification). The impedance of each resonator needs to be obtained in order to account for the effects of resonance. In order to calculate the impedance of a single Helmholtz resonator, the transfer matrix method is used. The full matrix, T, is derived from the following expression [11]:

$$T = M_n M_{\Delta l} M_c. \tag{30}$$

The transfer matrices for the neck, M_n, and the cavity, M_c, take the form of a standard fluid layer, represented in Eq. (16). The characteristic impedance and acoustic wavenumber of the neck and cavity for a cylindrical resonator are calculated using Eqs. (8) and (9). The transfer matrix for the length correction, $M_{\Delta l}$, is written as:

$$M_{\Delta l} = \begin{bmatrix} 1 & iZ_n k_n \Delta l \\ 0 & 1 \end{bmatrix}, \tag{31}$$

where Δl is arrived at from the addition of two correction lengths, $\Delta l = \Delta l_1 + \Delta l_2$. Δl_1 is due to pressure radiation at the discontinuity from the neck to the cavity [12] and Δl_2 comes from the pressure radiation at the discontinuity from the neck to the surrounding medium [13] given by:

$$\Delta l_1 = 0.82\left[1 - 1.35\frac{r_n}{r_c} + 0.31\left(\frac{r_n}{r_c}\right)^3\right] r_n \tag{32}$$

and

$$\Delta l_2 = 0.82\left[1 - 0.235\frac{r_n}{r_w} - 1.32\left(\frac{r_n}{r_w}\right)^2 + 1.54\left(\frac{r_n}{r_w}\right)^3 - 0.86\left(\frac{r_n}{r_w}\right)^4\right] r_n. \tag{33}$$

Here, r_w is the hydraulic radius of the waveguide, r_n is the neck radius and r_c is the cavity radius. To determine the characteristic impedance for the resonator, the final T matrix is multiplied by $[1, 0]^T$. This accounts for the velocity termination. Therefore, the characteristic impedance of the Helmholtz resonator at $x = 0$ can be found as follows:

$$Z_{HR} = \frac{P_{x=0}}{v_{x=0}} = \frac{T_{11}}{T_{21}}. \tag{34}$$

This yields the expression:

$$Z_{HR} = -i\frac{\cos(k_n l_n)\cos(k_c l_c) - Z_n k_n \Delta l \cos(k_n l_n)\sin(k_c l_c)/Z_c - Z_n \sin(k_n l_n)\sin(k_c l_c)/Z_c}{\sin(k_n l_n)\cos(k_c l_c)/Z_n - k_n \Delta l \sin(k_n l_n)\sin(k_c l_c)/Z_c + \cos(k_n l_n)\sin(k_c l_c)/Z_c}. \tag{35}$$

3. General model for effective material properties through TMM summation

The transfer matrix method provides a system of two equations which relates the acoustic pressure, p, and the volume flux, V, at $x = 0$ and $x = L$, where L is the length of the system. For a two-port system these are:

$$p_0 = T_{11}p_L + T_{12}V_L, \tag{36}$$

and

$$V_0 = T_{21}p_L + T_{22}V_L. \tag{37}$$

The subscripts 0 and L denote the respective variable value at $x = 0$ and $x = L$ of the system. Consider a system discretised into M segments, each with a cross section $S_a^{(m)}$ and length $l^{(m)}$, where (m) denotes the m^{th} segment. By applying the velocity–pressure relationship $V_L = p_L/Z_L$, where Z_L is the characteristic impedance at the local coordinate $x = L$ of a segment, Eqs. (36) and (37) can be modified to model the change in pressure and particle velocity within the m^{th} segment. These expressions are:

$$p_0^{(m)} = \left(T_{11}^{(m)} + \frac{T_{12}^{(m)}}{Z_L^{(m)}}\right)p_L^{(m)}, \tag{38}$$

and

$$v_0^{(m)} = \frac{1}{S_a}\left(T_{21}^{(m)} + \frac{T_{22}^{(m)}}{Z_L^{(m)}}\right)p_L^{(m)}. \tag{39}$$

For further clarification, Fig. 4 shows the m^{th} segment of an arbitrary system. Continuing this notion of a discretised system and utilising the equation of motion (1), the equation of motion for the m^{th} segment of a system can be described as:

$$-\left(\frac{\partial p}{\partial x}\right)^{(m)} = i\omega\rho(\omega)^{(m)}v^{(m)}. \tag{40}$$

Here the pressure gradient of the fluid within the m^{th} segment, $(\partial p\,/\partial x)^{(m)}$, can be expressed as $(p_L^{(m)} - p_0^{(m)})/l^{(m)}$, assuming $l^{(m)}$ is sufficiently small with respect to the wavelength. The average fluid velocity across the m^{th} segment, $v^{(m)}$, is taken to be $v_L^{(m)}$ to capture velocity variation along the segment. Assuming that the tortuosity of the m^{th} segment is equal to unity due to the constant cross section, by inputting these substitutions from Eqs. (38) and (39) and some algebraic manipulation, the effective dynamic density of the fluid within the m^{th} segment of a system can be obtained as:

$$\rho_{eff}^{(m)}(\omega) = \frac{\left((T_{11}^{(m)} - 1)Z_L^{(m)} + T_{12}^{(m)}\right)S_a^{(m)}}{i\omega l^{(m)}}. \tag{41}$$

To determine the effective density of the total system, the effective densities for all segments are superimposed. Each term is multiplied by the acoustic inertance weighting factor, $\left(l^{(m)}/S_a^{(m)}\right)/\sum_{m=1}^{M}\left(l^{(m)}/S_a^{(m)}\right)$, to account for density terms from narrow cross sections being dominant in the total effective dynamic density. The tortuosity of the total system, α_∞, is then included as a factor on the superimposed expression. This is defined as [14]:

$$\alpha_\infty = \frac{\sum_{m=1}^{M} S_a^{(m)} l^{(m)}}{\left(\sum_{m=1}^{M} l^{(m)}\right)^2}\sum_{m=1}^{M}\frac{l^{(m)}}{S_a^{(m)}}. \tag{42}$$

Therefore, the total effective density of the fluid within the system is calculated using the following expression:

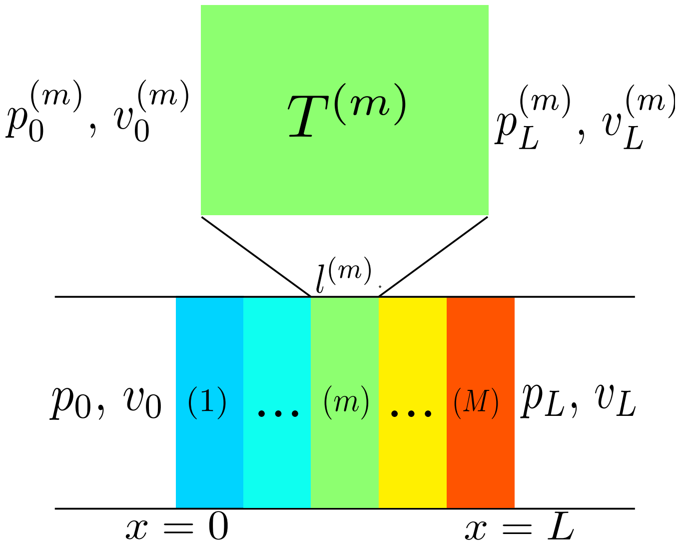

Fig. 4. Graphical depiction of the application of the modified transfer matrix equations to the m^{th} segment of an arbitrary system.

$$\rho_{eff}(\omega) = \frac{\alpha_\infty \sum_{m=1}^{M} \rho_{eff}^{(m)}(\omega) l^{(m)}/S_a^{(m)}}{\sum_{m=1}^{M} l^{(m)}/S_a^{(m)}} = \frac{\alpha_\infty \sum_{m=1}^{M} \left((T_{11}^{(m)} - 1) Z_L^{(m)} + T_{12}^{(m)} \right)}{\mathrm{i}\omega \sum_{m=1}^{M} l^{(m)}/S_a^{(m)}}. \quad (43)$$

Using the same logic and applying this to Eq. (4), the rate of change in the acoustic velocity for the fluid in the m^{th} segment can be described as:

$$-\left(\frac{\partial v}{\partial x}\right)^{(m)} = \mathrm{i}\omega C(\omega)^{(m)} p^{(m)}. \quad (44)$$

Here, the velocity gradient of the fluid within the m^{th} segment $(\partial v/\partial x)^{(m)}$ can be expressed as $(v_L^{(m)} - v_0^{(m)})/l^{(m)}$, where $v_L^{(m)} = p_L^{(m)}/(Z_L^{(m)} S_a)$, assuming $l^{(m)}$ is sufficiently small with respect to the wavelength. The acoustic pressure $p^{(m)}$ is taken to be $p_L^{(m)}$ to capture pressure variation along the segment. Again, by inputting these substitutions from Eqs. (38) and (39), the following expression can then be obtained for the effective complex compressibility of the fluid in the m^{th} segment of a system:

$$C_{eff}^{(m)}(\omega) = \frac{T_{21}^{(m)} Z_L^{(m)} + T_{22}^{(m)} - 1}{\mathrm{i}\omega l^{(m)} Z_L^{(m)} S_a^{(m)}}. \quad (45)$$

By multiplying the effective complex compressibility of the fluid within each segment by the volumetric weighting factor, $S_a^{(m)} l^{(m)} / \sum_{m=1}^{M} S_a^{(m)} l^{(m)}$, to account for compressibility terms from large cross sections being dominant in the total effective complex compressibility, and superimposing all terms, the total effective complex compressibility of the fluid within the system can be expressed as:

$$C_{eff}(\omega) = \frac{\sum_{m=1}^{M} C_{eff}^{(m)}(\omega) S_a^{(m)} l^{(m)}}{\sum_{m=1}^{M} S_a^{(m)} l^{(m)}} = \frac{\sum_{m=1}^{M} \left(T_{21}^{(m)} Z_L^{(m)} + T_{22}^{(m)} - 1 \right) \left(Z_L^{(m)} \right)^{-1}}{\mathrm{i}\omega \sum_{m=1}^{M} S_a^{(m)} l^{(m)}}. \quad (46)$$

A simple approach is now available to obtain analytical expressions for systems modelled by the TMM. The above expressions can be used to assess how the complex compressibility, dynamic density, speed of sound, effective wavenumber and characteristic impedance varies within a complex system.

4. Effective material properties of a rigid frame porous material

A simple theoretical model that describes the sound propagation through pores of known cross-sectional area and shape is proposed by Champoux and Stinson in Ref. [9]. A brief outline of this method is presented in Section 2.3. This same rigid pore system is modelled using the proposed TMM summation method and results are compared with those from the TMM multiplication method.

4.1. Application of the TMM summation method to model a rigid frame porous material

Consider a single pore composed of M distinct cylindrical segments which are constant in cross section. Each segment, m, has a length $l^{(m)}$ and a radius $r^{(m)}$ (see Fig. 1 for a schematic of this geometry). The total transfer matrix of the system, T, is:

$$T = M_\Omega \cdot M^{(1)} \cdot M^{(2)} \ldots M^{(M-1)} \cdot M^{(M)} \cdot M_\Omega^{-1}, \quad (47)$$

where $M^{(m)}$ is the transfer matrix for the m^{th} segment fluid layer. Here, the acoustic wavenumber, $k^{(m)}$, and characteristic impedance, $Z^{(m)}$, are obtained with Eqs. (8) and (9) to account for the viscothermal losses of each segment. M_Ω accounts for the porosity of the system and is defined as:

$$M_\Omega = \begin{bmatrix} 1 & 0 \\ 0 & \frac{1}{\Omega} \end{bmatrix}. \quad (48)$$

From this total matrix, the effective fluid properties can be obtained by with the TMM multiplication method using Eqs. (18) and (19).

For the TMM summation method, the effective density and compressibility of the system can be obtained by utilising Eqs. (43) and (46) upon each matrix in the system. This results in the following expressions:

$$\rho_{eff}(\omega) = \frac{\alpha_\infty \sum_{m=1}^{M} \left(\cos\left(k^{(m)} l^{(m)}\right) + \mathrm{i}\sin\left(k^{(m)} l^{(m)}\right) - 1 \right) Z^{(m)}}{\mathrm{i}\omega \sum_{m=1}^{M} \left(l^{(m)}/S_a^{(m)} \right)} \quad (49)$$

and

$$C_{eff}(\omega) = \frac{\sum_{m=1}^{M} \left(\cos\left(k^{(m)} l^{(m)}\right) + \mathrm{i}\sin\left(k^{(m)} l^{(m)}\right) - 1 \right) \left(Z^{(m)} \right)^{-1}}{\mathrm{i}\omega \sum_{m=1}^{M} \left(S_a^{(m)} l^{(m)} \right)}. \quad (50)$$

By taking the low frequency limit, $k^{(m)}l^{(m)} \ll 1$, the series expansion of the common expression present in Eqs. (49) and (50) can be calculated. The result of this is:

$$\cos\left(k^{(m)}l^{(m)}\right) + \mathrm{i}\sin\left(k^{(m)}l^{(m)}\right) - 1 = \mathrm{i}k^{(m)}l^{(m)} + \mathcal{O}\left\{\left(k^{(m)}l^{(m)}\right)^2\right\}. \quad (51)$$

Therefore, utilising the leading order term from the series expansion, the total dynamic density and complex compressibility of the fluid within the tortuous pore can be defined as:

$$\rho_{eff}(\omega) = \alpha_\infty \frac{\sum_{m=1}^{M} \rho(\omega)^{(m)} l^{(m)} / S_a^{(m)}}{\sum_{m=1}^{M} l^{(m)} / S_a^{(m)}} \quad (52)$$

and

$$C_{eff}(\omega) = \frac{\sum_{m=1}^{M} C(\omega)^{(m)} S_a^{(m)} l^{(m)}}{\sum_{m=1}^{M} S_a^{(m)} l^{(m)}}, \quad (53)$$

where $\rho(\omega)^{(m)}$ and $C(\omega)^{(m)}$ are the dynamic density and complex compressibility of the fluid in the m^{th} segments calculated with Eqs. (8) and (9). It can be seen that these expressions match the Champoux and Stinson model.

4.2. Results

In this section, a single pore of four distinct segments of varying cross section is modelled using the proposed TMM summation method and then validated against the traditional TMM multiplication method. The geometric parameters for the pore can be seen in Table 1. The resulting tortuousity of the system is $\alpha_\infty = 3.26$ and the sample cross sectional area can be selected as an arbitrary

Table 1
Geometric properties of rigid framed pore structure. All units are [mm].

$r^{(1)}$	$r^{(2)}$	$r^{(3)}$	$r^{(4)}$	$l^{(1)}$	$l^{(2)}$	$l^{(3)}$	$l^{(4)}$	L
2	0.75	3	1.5	1	2.5	2	1	6.5

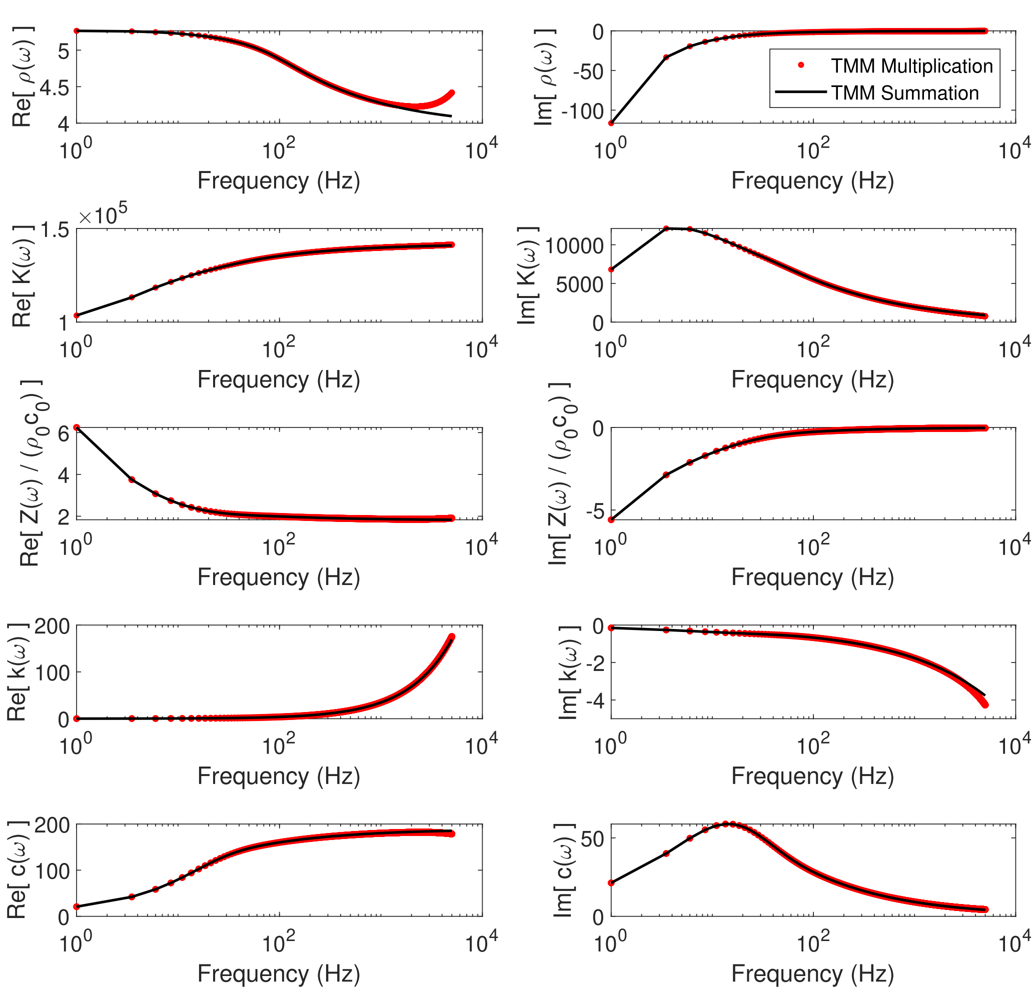

Fig. 5. The effective density $\rho(\omega)$ [kg/m^3], bulk modulus $K(\omega)$ [Pa], normalised acoustic impedance $Z(\omega)$, wavenumber $k(\omega)$ [1/m] and speed of sound $c(\omega)$ [m/s] computed using the proposed effective property model (TMM summation) and the traditional TMM method (TMM Multiplication).

value as the above methods obtain the effective properties for the fluid within the pore. The plots of the real and imaginary components of effective material properties, normalised acoustic impedance, wavenumber and speed of sound can be seen in Fig. 5.

From Fig. 5 it is evident that there is excellent agreement between the TMM summation and TMM multiplication models in the low frequency regime, with a mean absolute percentage error (MAPE) of 0.6% for the effective density and MAPE of 0.032% for the effective bulk modulus, within the first 1000 Hz. Past this it can be seen that the two methods begin to deviate from one another, as evidenced in the dynamic density and wavenumber of this system. As Eqs. (52) and (53) are experimentally validated by Champoux and Stinson [9], with a similar pore geometry for up to 5 kHz, it is thought this deviation is associated with a limitation in the retrieval of the effective properties using the TMM multiplication method. Finally, if one wanted to increase the scale of the system by an order of magnitude whilst retaining the same tortuousity, radiation effects would then have to be accounted for [15]. This approach can be implemented with additional transfer matrices for the TMM summation and mutliplication methods.

5. Effective material properties of a waveguide sideloaded by Helmholtz resonators

In this section, the effective fluid properties are obtained for a waveguide sideloaded by M Helmholtz resonators. This is done using the TMM summation method presented within Section 3. The obtained effective fluid properties are compared with those obtained using the TMM multiplication method presented in Section 2.4.2.

5.1. Application of the TMM sumattion method to model a waveguide sideloaded by Helmholtz resonators

Consider a waveguide section of constant cross-section, S_a, and length, L, side-loaded by M Helmholtz resonators periodically space by $l = L/(M-1)$. As shown in Fig. 6. The transfer matrix for the whole system is expressed as:

$$T = M_{HR}^{(1)} \cdot M_{WG} \cdot M_{HR2}^{(2)} \dots M_{WG} \cdot M_{HR}^{(M-1)} \cdot M_{WG} \cdot M_{HR}^{(M)}, \tag{54}$$

where the waveguide transfer matrix, M_{WG}, is the transfer matrix of a fluid layer of length l. Within this matrix, $Z = \rho c/S_a$, is the characteristic impedance for plane wave propagation within the fluid of the waveguide, and k is the wavenumber of the fluid within the waveguide. These quantites are determined with the use of Eqs. (10) and (11). The resonators are introduced as point scatterers within the transfer matrix, which is facilitated for the m^{th} resonator by the following matrix:

$$M_{HR}^{(m)} = \begin{bmatrix} 1 & 0 \\ \frac{1}{Z_{HR}^{(m)}} & 1 \end{bmatrix}. \tag{55}$$

To calculate the effective material properties using the traditional method of matrix multiplication, it is a simple manner of utilising the equations set out in Section 2.4.2 upon the final transfer matrix, T, of the system.

Through the application of Eq. (43) upon the transfer matrices in Eq. (54), the total effective dynamic density of the fluid within the system can be explicitly written as:

$$\rho_{eff}(\omega) = \frac{ZS_a}{\mathrm{i}\omega L}\sum_{m=1}^{M-1}(\cos(kl) + \mathrm{i}\sin(kl) - 1). \tag{56}$$

Through the application of Eq. (46) upon the transfer matrices in Eq. (54), the total effective compressibility of the fluid within the system can be explicitly expressed as:

$$C_{eff}(\omega) = \frac{1}{\mathrm{i}\omega LS_a}\left\{\frac{1}{Z}\sum_{m=1}^{M-1}(\cos(kl) + \mathrm{i}\sin(kl) - 1) + \sum_{m=1}^{M}\frac{1}{Z_{HR}^{(m)}}\right\}. \tag{57}$$

By taking the low frequency limit, $kl \ll 1$, the total dynamic density and complex compressibility of the fluid within the system can be defined as:

$$\rho_{eff}(\omega) = \rho(\omega), \tag{58}$$

$$C_{eff}(\omega) = C(\omega) + \frac{1}{\mathrm{i}\omega LS_a}\sum_{m=1}^{M}\frac{1}{Z_{HR}^{(m)}}, \tag{59}$$

where $\rho(\omega)$ and $C(\omega)$ are the dynamic density and complex compressibility of the waveguide.

5.2. Results

To assess the validity of Eqs. (58) and (59), a system of two cylindrical Helmholtz resonators side-loading a square waveguide is modelled. This system contains two distinct resonances resulting from variation in geometry between the Helmholtz resonators. Namely, a difference in the cross sectional area of the necks. A limiting factor in using an effective fluid layer transfer matrix to compute the reflection coefficient is due to the assumption that the system is a symmetric absorber, i.e. $T_{11} = T_{22}$. When this is not the case, such as in a degenerate coupling of Helmholtz resonators [16], the use of effective properties as presented within this paper is unfit for purpose in obtaining the reflection and absorption coefficients. This does not apply to the transmission coefficient due to the reciprocal nature of this type of system, i.e. $T_{11}T_{22} - T_{12}T_{21} = 1$.

As such, the following example has been selected as to minimise asymmetry in the reflection coefficient. This has been done with an asymmetric geometry which is possible due to very weak

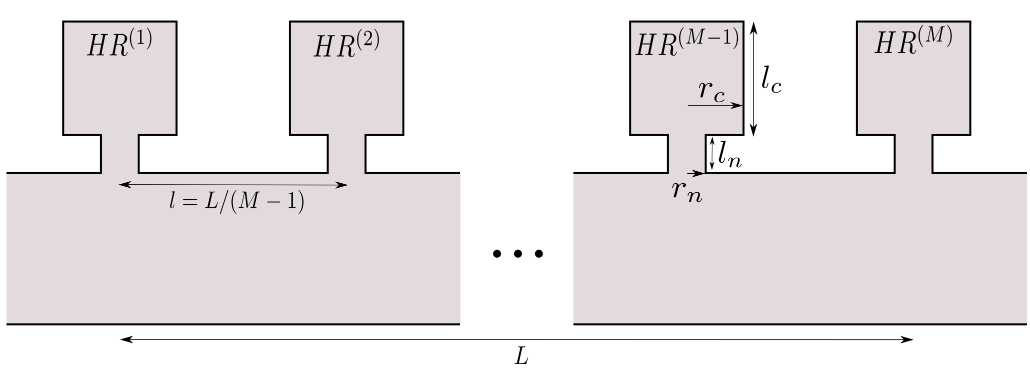

Fig. 6. Schematic for a system of M equispaced cylindrical HRs sideloading a square waveguide.

Table 2
Geometric properties of the modelled Helmholtz resonators. All units are [mm].

HR	r_n	r_c	l_n	l_c
1	3	15	10	40
2	1.5	15	10	40

coupling between the Helmholtz resonators. The length of the system is $L = 34mm$, the width, a, and height, b, of the waveguide are $a = b = 50mm$. The geometry of the modelled Helmholtz resonators can be seen in Table 2 with these quantities graphically represented in Fig. 6.

The plots of the effective dynamic density, effective bulk modulus, normalised acoustic impedance, acoustic wavenumber and the speed of sound computed using the effective property model and the TMM multiplication method can be seen in Fig. 7. From Fig. 7 it is evident that there is good agreement in all terms, although fluctuations within the effective density are evident in the TMM multiplication model which have not been captured with the TMM summation model. The physical nature of these fluctuations is uncertain and could either be a result of the resonances of the Helmholtz resonators or numerical errors in the retrieval of the effective wavenumber and impedance with the TMM multiplication method. Nonetheless, it can be seen that these fluctuations play no significant role in subsequent terms derived from the dynamic density and as such, regardless of the physical meaning of these fluctuations, they can be deemed negligible. To support this, the effective dynamic density has a MAPE of 2.4% and the effective bulk modulus also has a MAPE of 2.4%. Therefore, the TMM summation model can be deemed as a valid approach to derive analytical approximations for symmetric or near-symmetric systems composed of Helmholtz resonators. To corroborate this claim, it has been shown that through the use of the modal expansion method [17], an analytical approximation for the effective dynamic density of a waveguide side-loaded by Helmholtz resonators matches that of Eq. (58) obtained using the TMM summation method.

The transmission, reflection and absorption coefficients of the system have been computed using the TMM method, numerically and with the TMM summation method. The equations used to obtain the transmission and reflection coefficients were (28) and (29). These equations were applied to the total transfer matrix of the system for the TMM method and to the transfer matrix of an effective fluid layer for the TMM summation method. The numerical calculations were done using COMSOL 5.0 using the Acoustics Pressure Module. The model was 3D with the viscothermal losses being accounted for in every region of the structure. The system used for the computation had two Intel(R) Xeon(R) 8 core CPUs @2.60 GHz with 128 GB of RAM. The plots of these coefficients

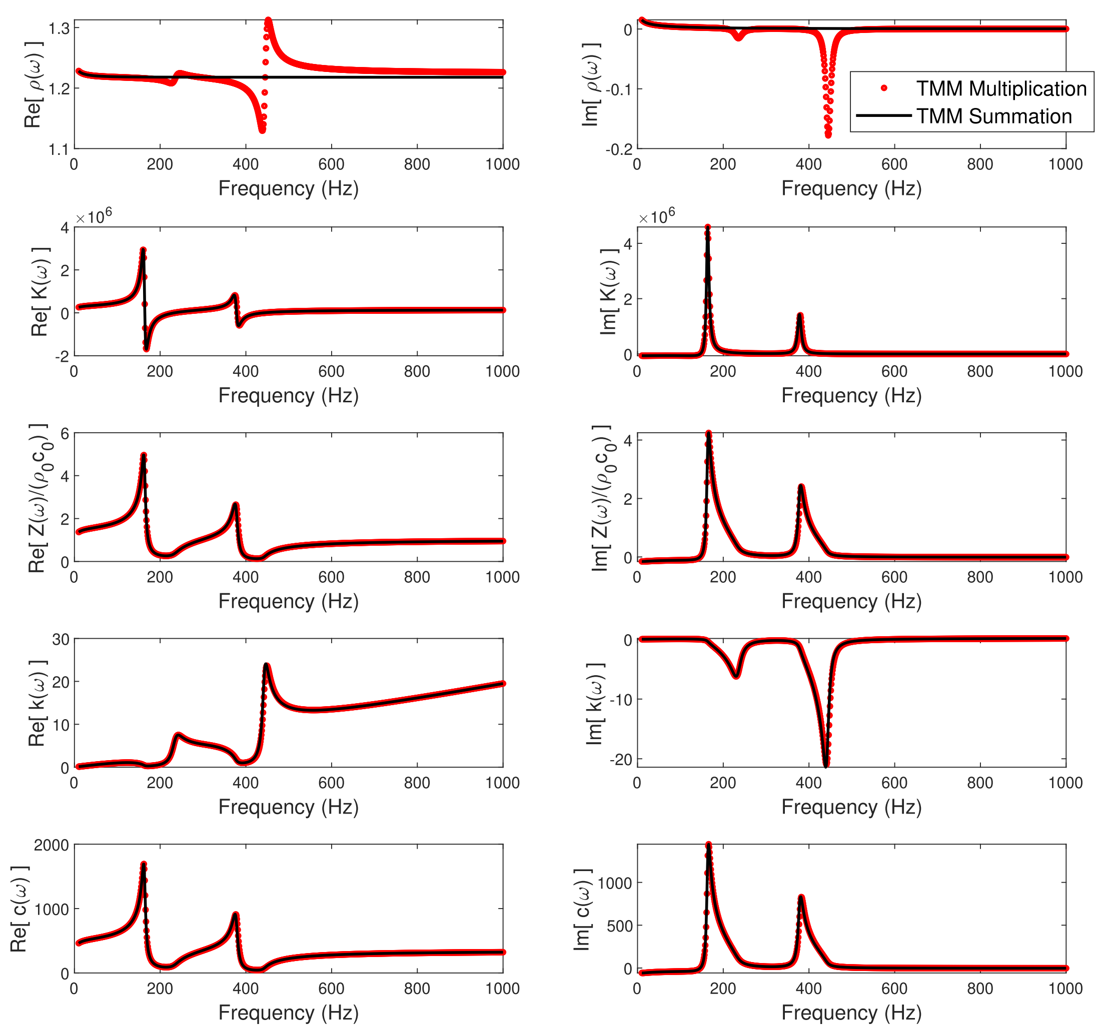

Fig. 7. The effective dynamic density $\rho(\omega)$ [kg/m^3], effective bulk modulus $K(\omega)$ [Pa], normalised impedance $Z(\omega)$, acoustic wavenumber $k(\omega)$ [1/m] and speed of sound $c(\omega)$ [m/s] computed using the effective property model (TMM summation) and the traditional TMM method (TMM Multiplication).

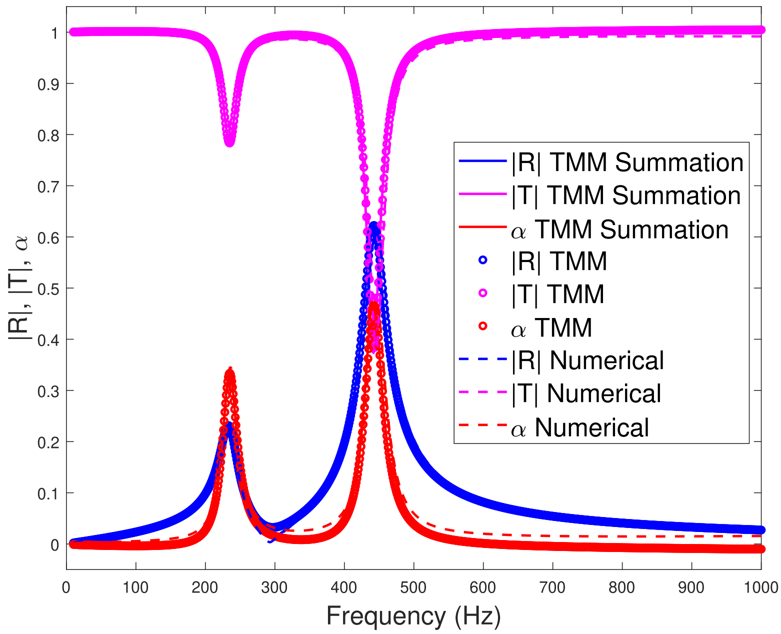

Fig. 8. The transmission ($|T|$), reflection ($|R|$) and absorption (α) coefficients computed using the effective property model (TMM summation) in comparison to the coefficients obtained with the traditional TMM method (TMM) and numerically (Numerical).

Table 3
Geometric properties of the modelled degenerate Helmholtz resonators. All units are [mm].

HR	r_n	r_c	l_n	l_c
1	4	15	10	40
2	4	15	10	42

for the three methods can be seen in Fig. 8. From Fig. 8 it is evident that there is good agreement between the three methods when computing the transmission properties of the selected system. Due to the near-symmetry in the system, it can be seen that the reflection and absorption coefficients obtained with the TMM summation method remains consistent with the coefficients obtained using the TMM and numerical methods. From the results it can be concluded that the TMM summation method provides valid analytical approximations to the traditional TMM method, so long as the modelled system does not exhibit asymmetric reflection properties and L is not too large compared to the wavelength.

It must be noted that this model only remains valid in the low frequency regime, below the first Bragg frequency and the first cross sectional mode of the waveguide. This is due to the models inability to account for effects associated with periodicity and the assumption of plane wave propagation within the formulation of the model. The failure to capture effects due to periodicity can be seen upon examination of Eq. (59) where the summation term associated with each resonator is scaled by the total length of the system, not the separation of each resonator.

To highlight the inability to capture asymmetric reflection phenomenon using the two effective property models presented here, a set of degenerate Helmholtz resonators have been modelled using the TMM, TMM summation and TMM multiplication methods. The geometry of the Helmholtz resonators can be found in Table 3. The waveguide dimensions and system length are unchanged. The plots of the absorption coefficient for the two directions of incidence, α^+ and α^-, obtained with the TMM method, absorption coefficients obtained using the TMM summation method and TMM multiplication method are presented in Fig. 9. From Fig. 9 it can be seen that when using the TMM method, the effects of strong evanescent coupling can be captured. This is evident with the large disparity between the amplitude of absorption between the two directions of incidence. Adversely, when looking at the plots produced by the two effective property methods, there is little correlation to the absorption for either direction of incidence. Additionally, there is poor agreement between the two effective property models too. As such, the two effective property models are only valid for systems of Helmholtz resonators in which there is weak evanescent coupling. If evanescent coupling were to be captured, the effective fluid properties would have to be modified for each direction of incidence.

6. Conclusion

A general effective property model has been proposed to obtain explicit analytical expressions for complex systems. By discretising a system into segments, it is possible to utilise the transfer matrix method to predict the acoustic properties in these segments. Through the application of linear superposition, these individual segment effective properties can be summated to achieve the total effective properties of the system. Analytical expressions were derived for two use in order to validate the model.

Firstly, the proposed approach was applied to derive the effective properties for the fluid in a singular pore consisting of M unique cylindrical cross sections. This is consistent with the well established Champoux-Stinson model for rigid pored structures. These expressions were then used to describe the dynamic behaviour of the fluid in a pore of four segments with varying radii and lengths. The results of this method were also compared with those obtained with a conventional TMM formulation. It was found upon examination of all effective properties that there is excellent agreement between the two models in the low-frequency regime.

Subsequently, using the same methodology, the effective properties for a waveguide side-loaded by M Helmholtz resonators were derived. To validate the expressions, the effective fluid properties of a waveguide side-loaded by two HRs obtained with the TMM summation method were compared with those obtained

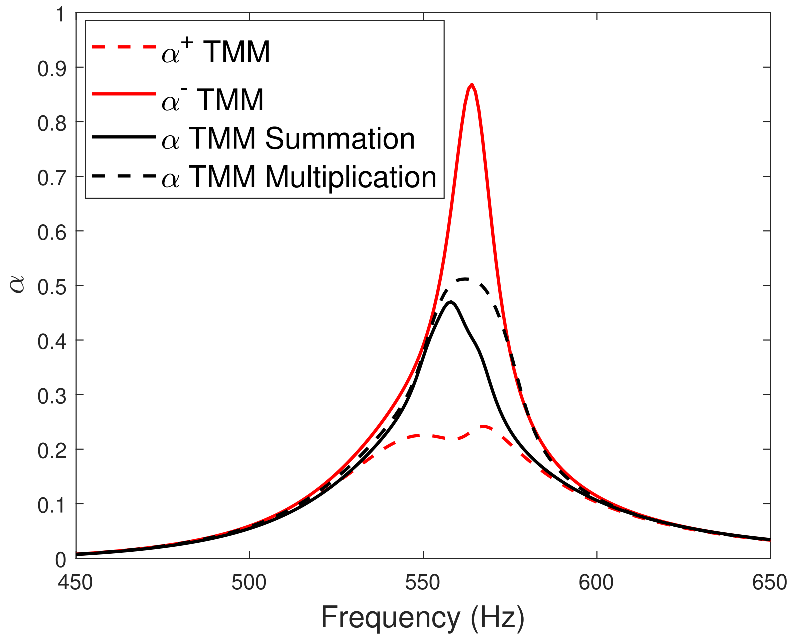

Fig. 9. Plots of the absorption coefficient for the two directions of incidence α^+ and α^-, obtained with the TMM method, against the absorption coefficient obtained using the TMM summation and multiplication methods.

via the TMM multiplication method. It was found that there is excellent agreement in all terms except the effective dynamic density. It is thought these fluctuations are the result of numerical error and possess no physical meaning. Nonetheless, the influence these fluctuations play on subsequent terms is negligible. Additionally, the transmission properties obtained through the effective property model were compared with those obtained through the traditional TMM and a numerical FEM model. The selected geometry was asymmetric but it exhibited near-symmetric reflection properties due to the weak evanescent coupling of the Helmholtz resonators. It was found that there was excellent agreement between the methods.

CRediT authorship contribution statement

A. Dell: Conceptualization, Methodology, Writing - original draft, Writing - review & editing. **A. Krynkin:** Methodology, Writing - review & editing. **K.V. Horoshenkov:** Writing - review & editing.

Declaration of Competing Interest

The authors declare that they have no known competing financial interests or personal relationships that could have appeared to influence the work reported in this paper.

Acknowledgments

The authors are grateful for the financial support of the doctoral training grant provided by the department of mechanical engineering at the University of Sheffield and the UK Engineering and Physical Sciences Research Council (EPSRC) grant EP/N509735/1. A. Dell is grateful for the financial support of Sonobex Ltd. The authors would also like to thank the anonymous reviewers for their helpful comments on improving the paper.

References

[1] Seo Sang-Hyun, Kim Yang-Hann. Silencer design by using array resonators for low-frequency band noise reduction. J Acoust Soc Am 2005;118(4):2332–8.
[2] Bradley CE. Time harmonic acoustic bloch wave propagation in periodic waveguides. Part i. Theory. J Acoust Soc Am 1994;96(3):1844–53.
[3] Theocharis G, Richoux O, Romero García V, Merkel A, Tournat V, et al. Limits of slow sound propagation and transparency in lossy, locally resonant periodic structures. New J Phys 2014;16(9):093017.
[4] Song Bryan H, Stuart Bolton J. A transfer-matrix approach for estimating the characteristic impedance and wave numbers of limp and rigid porous materials. J Acoust Soc Am 2000;107(3):1131–52.
[5] Jean Noureddine Atalla, Allard F. Propagation of sound in porous media. John Wiley & Sons; 2009.
[6] Verdière Kévin, Panneton Raymond, Elkoun Saïd, Dupont Thomas, Leclaire Philippe. Transfer matrix method applied to the parallel assembly of sound absorbing materials. J Acoust Soc Am 2013;134(6):4648–58.
[7] Romero-García V, Theocharis G, Richoux O, Merkel A, Tournat V, Pagneux V. Perfect and broadband acoustic absorption by critically coupled sub-wavelength resonators. Scientific Rep 2016;6(1).
[8] Jiménez Noé, Romero-García Vicent, Pagneux Vincent, Groby Jean-Philippe. Rainbow-trapping absorbers: Broadband, perfect and asymmetric sound absorption by subwavelength panels for transmission problems. Scientific Rep 2017;7(1):13595.
[9] Champoux Yvan, Stinson Michael R. On acoustical models for sound propagation in rigid frame porous materials and the influence of shape factors. J Acoust Soc Am 1992;92(2):1120–31.
[10] Stinson Michael R. The propagation of plane sound waves in narrow and wide circular tubes, and generalization to uniform tubes of arbitrary cross-sectional shape. J Acoust Soc Am 1991;89(2):550–8.
[11] Richoux O, Pagneux V. Acoustic characterization of the hofstadter butterfly with resonant scatterers. Europhys Lett 2002;59(1):34–40.
[12] Kergomard J, Garcia A. Simple discontinuities in acoustic waveguides at low frequencies: Critical analysis and formulae. J Sound Vib 1987;114(3):465–79.
[13] Dubos V, Kergomard Jean, Khettabi Ali, Dalmont Jean-Pierre, Keefe DH, Nederveen CJ. Theory of sound propagation in a duct with a branched tube using modal decomposition. Acta Acust United Acust 1999;85:153–69.
[14] Horoshenkov Kirill V, Hurrell Alistair, Groby Jean-Philippe. A three-parameter analytical model for the acoustical properties of porous media. J Acoust Soc Am 2019;145(4):2512–7.
[15] King PDC, Cox TJ. Acoustic band gaps in periodically and quasiperiodically modulated waveguides. J Appl Phys 2007;102(1):014902.
[16] Merkel A, Theocharis G, Richoux O, Romero-García V, Pagneux V. Control of acoustic absorption in one-dimensional scattering by resonant scatterers. Appl Phys Lett Dec 2015;107(24):244102.
[17] Jiménez N, Huang W, Romero-García V, Pagneux V, Groby J-P. Ultra-thin metamaterial for perfect and quasi-omnidirectional sound absorption. Appl Phys Lett 2016;109(12):121902.